

# Roof Tunnel Stability by Wedge Analysis

Mehdi Zamani Lenjani, Ali Nikjo

Department of Civil Engineering, Yasouj University

Received: 2017/12/04

Accepted: 2019/01/01

## Abstract

A jointed rock mass presents a more complex design problem than the other rock masses. The complexity arises from the number (greater than two) of joint sets which define the degree of discontinuity of medium. The condition that arises in these types of rock masses is the generation of discrete rock blocks, of various geometries. They are defined by the natural fracture surfaces and the excavation surface. Stability problems in blocky jointed rock are generally associated with gravity falls of blocks from the roof and sidewalls. Whereas for block defined in the crown of tunnel, the requirement is to examine the potential for displacement of each block under the influence of the surface tractions arising from the local stress field and the gravitational load, in this paper various types of wedge formation in the crown of tunnel due to intersection of joint sets with various dip were examined. The state of stability of the wedge was then assessed through the factor of safety against roof failure. Following that the formed wedges in New York city and Washington D.C tunnel crowns was investigated with limit equilibrium analytical method and by use of Hoek and Brown failure criterion. The obtained results from analytical method corresponded with field observation.

**Keywords** Limit equilibrium, Stability analysis, Joint set, Rock mass, Wedge

## Introduction

Excavations cut into rock masses with several sets of discontinuities may release rock blocks of various sizes. The potential movements of the most critically located of these may then undermine adjacent blocks, and the ensuing block falls and slides can menace the integrity of the engineering scheme. If the excavation is unsupported, block movements may unacceptably alter the excavation perimeter and the blocks may cause property damage and personal injury. If the excavation has been supported, the block movement tendency will transfer loads to the support system,

---

\*Corresponding author      mahdi@yu.ac.ir

which could fail if they have not been designed specifically to handle these loads. Suppose that a block of rock is isolated by the intersection of discontinuities and excavation surfaces. No matter how many faces it has, the block can move initially in only a few ways: by falling, by sliding on one face, or by sliding on two faces (or by combined sliding and rotation). All these movements require that certain faces open. Thus, the first warning of block movement is the widening of particular joints. On the other hand, if potentially dangerous blocks are found prior to movement and their stability is assured, then no block movements will occur anywhere and the excavation stability will be assured. The stability of a block or wedge of rock in a discontinuous rock mass has been studied analytically by many researchers, mainly based on the limit equilibrium approach.

Bray [1] proposed an analysis of a symmetric wedge present in the roof of an underground opening. The material comprising the body of the wedge was assumed rigid, all deformations being restricted to the bounding discontinuity planes. John [2], Londe et al. [3], Hendron et al. [4], Hoek and Bray [5], Warburton [6], Priest [7], and Goodman and Shi [8] considered sliding modes only and the mode must be assumed a priori. Chan and Einstein [9], Mauldon and Goodman [10] and Tonon [11] considered special cases of rotation and discussed the rotational stability of a rock block. But they stopped short of providing a procedure that can handle general modes of simultaneous sliding and rotation. A review of existing limit equilibrium-based wedge stability analysis methods shows that (1) they do not consider dynamic equilibrium, (2) most cannot handle rotational modes, and (3) none can handle complicated rotational modes such as torsional sliding. Different researchers defined the factor of safety of the rock block in different ways. For example, Sofianos [12], Sofianos et al. [13], Nomikos et al. [14], and Hudson and Harrison [15] defined the factor of safety FS1 as the ratio of the resultant of all forces applied to the block (except for its weight) to the weight of the block.

Unwedge [16] defines the factor of safety FS2 as the ratio of passive to active forces. The same definition was used in BS3D [17] (a computer code developed based on single rock block stability algorithm proposed by Tonon [18] and validated for wedge failure [19]). Definition of factor of safety for rock blocks is investigated by Asadollahi and Tonon [20]. Wang and Yin [21] and Chen [22] proposed a general formulation for rock wedge stability analysis by using an upper bound method and considering the dilatancy of discontinuities.

Yeung et al. [23] developed a three-dimensional discontinuous deformation analysis (3D DDA) procedure for the analysis of wedge

stability. This method was found capable of handling general modes of simultaneous sliding and rotation.

Probabilistic analysis has been widely used to quantify and model the variability and uncertainty of discontinuities [24-28]. In a probabilistic analysis, most of the geometrical and mechanical parameters of discontinuities are considered as random variables and types of distribution functions for each random variable need be selected carefully. However, there is a lack of consensus on these choices, which could lead to very different analysis results. Duncan and Christopher [29] pointed out that the analysis using the orientations other than the mean values may show that some unstable wedges can be formed (p. 64). Therefore, it is necessary to optimize analysis of wedge stability to locate the most dangerous wedge and its critical failure surface.

Qinghui Jiang et al presented a new method for analyzing the stability of rock wedges. This involves a genetic algorithm (GA) for searching the critical failure surface with the minimum factor of safety and provides a low-limit solution with conservative advantages for engineering support design to ensure the stability and safety of the rock slope [30].

Mirzaeian et al. [31] applied a kind of stochastic model TuPSA (Tunnel probabilistic structural analysis) using FORM (first order reliability model) in analysis of wedge stability around circular tunnel. They considered three joint sets with normal distribution of their strike and dip directions. The strength properties of joint surface such as cohesion and internal friction angle were also assumed to have normal distributions. The Mohr-Coulomb failure criterion was applied for stability of wedge. However that failure criterion is more applicable to soils whereas rock masses or intact rock the Hoek and Brown failure criterion is more appropriate. Curran et al. [32], by method of numerical Boundary element method and using Rocscience software, applied three-dimensional stability analysis of rock wedges around noncircular tunnel. The point with their research is the consideration of in-situ stresses in analysis. For simplicity Mohr-Coulomb failure criterion is used. Budiman et al. [33], for the stability of tunnel portal in open pit Aneka Tambang mine used RMR and SMR experimental approaches. Their research was more about stability analysis of mine slopes rather than the stability of tunnel portal. A rock block in the crown of an excavation is subject to its own weight,  $W$ , surface forces associated with the prevailing state of stress, and possibly fissure water pressure and some support load. The block surface forces can be determined by some independent analytical procedure, and that the block weight can be determined from the joint orientations and the excavation geometry. Stable,

continuous behavior of a jointed or granular medium exploits frictional resistance to shear stress, and this resistance is mobilized by tensile normal stress. Thus, generation and maintenance of a state of mechanically sustainable tensile stress in the excavation boundary rock, which may involve the installation of support and reinforcement, is a basic objective of design in this type of medium. When the gravitational weight of the wedge is high enough to overcome the frictional resistance of the plane or planes on which sliding would take place, the wedge is stable against sliding and otherwise the wedge is unstable. Joints are usually present in rock outcrops. They appear as approximately parallel planar cracks separated by several centimeters up to as much as 10m. One set of joints commonly forms parallel to bedding planes and there are usually at least two other sets in other directions. Igneous and metamorphic rocks may have regular jointing systems with three or more sets. Rocks that have been deformed by folding often contain roughly parallel seams of sheared and crushed rock produced by interlayer slip or minor fault development. These shears are usually spaced more widely than joints and are marked by several millimeters to as much as a meter thickness of soft or friable rock or soil. The locations of joints have affected the shape of the tunnel. From the intersection of the joint sets wedges are formed in tunnel crown. In some cases falling of these wedges is possible. (according to figures 1 and 2).

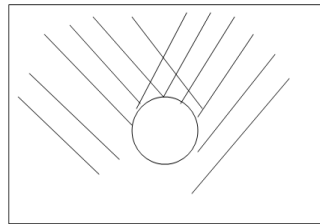


**Figure 1. The presence of two joint sets around a tunnel**

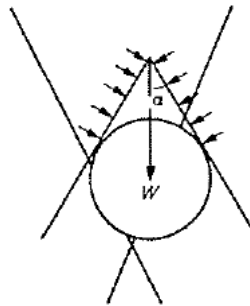


**Figure 2. The maximum size of formed wedge in tunnel crown**

Following that four states of wedges formed in tunnel crown are investigated and for each, the factor of safety against roof failure was calculated.

## Types of the wedges formed in tunnel crown

When the joint sets have equal dip and are in the opposite direction with free surface symmetric wedge (according to figure 3), and when the joint sets have unequal dip and are in the opposite direction with free surface asymmetric wedge will be formed (according to figure 5). Vertical wedge is formed when at least one of the joint set is vertical (according to figures 7) and sliding wedge will be formed when the joint sets have dips in one direction toward left or right (according to figure 8). In all the above cases free surface is toward tunnel and since stability of wedge formed in tunnel crown is investigated the base of the wedge is its free surface.

### 1. Symmetric falling roof wedge

#### 1-1. Symmetric falling roof wedge with vertical reaction force

Having identified the feasible block collapse modes associated with joint orientations and excavation surface geometry, it is necessary to determine the potential for block displacement under the conditions that will exist in the post-excavation state of the boundary of the opening. A rock block in the crown of an excavation is subject to its own weight,  $W$ , surface forces associated with the prevailing state of stress, and possibly fissure water pressure and some support load. The block surface forces can be determined by some independent analytical procedure, and that the block weight can be determined from the joint orientations and the excavation geometry. [34]

Figure (3) represents the cross section of a long, uniform, triangular wedge generated in the crown of an excavation by symmetrically inclined joints. The apical angle of the prism is  $2\theta$ . Considering unit thickness of the problem geometry in the antiplane direction, the block is acted on by its weight  $W$  and normal and shear forces  $N$  and  $S$  on its superficial contacts with the adjacent origin rock. To assess the stability analysis of the wedge, it is assumed that  $W$  force is replaced by two  $F$  forces acting on the lateral edges. Based on force equilibrium in  $y$ -direction can be written:

$$\sum F_y = 0 \rightarrow F = \frac{W}{2} \quad (1)$$

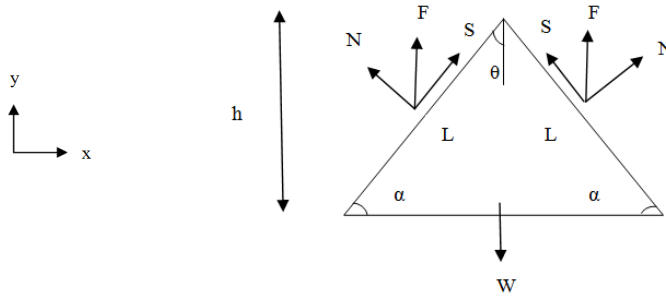


**Figure 3. Symmetric falling roof wedge**

Then by resolving the  $F$  force into two  $N$  tensile and  $S$  shear components, they are obtained by Equations (2).

$$N = -F \sin \theta \quad , \quad S = F \cos \theta \quad (2)$$

Considering unit thickness of the wedge in the antiplane direction,  $\sigma$  the normal tensile stress and  $\tau$  the shear stress are determined by Equation (3).

$$\sigma = \frac{N}{L \times 1} \quad , \quad \tau = \frac{S}{L \times 1} \quad (3)$$

In which  $L$  is the joint length.

After that by use of the approximate equations which are defining the relationships between principal stress and the Mohr envelopes for the failure of intact rock specimens and of heavily jointed rock masses, limiting state of shear stress is obtained. These equations are presented by Hoek and Brown for various types of rocks and are used for approximate failure analysis of rock. By representing the intact rock and then obtain the rock mass quality designation index by use of Bieniawski or Barton Classification Systems, appropriate equation is chosen for calculate the normalized principal stress or normalized shear stress. It should be noted that On the basis of an evaluation of a large number of case histories of underground excavations, Barton et al. (1974), of the Norwegian Geotechnical Institute proposed a Tunneling Quality Index ( $Q$ ) for the determination of rock mass characteristics and tunnel support requirements. The numerical value of the index  $Q$  varies on a logarithmic scale from 0.001 to a maximum of 1,000. Tunneling Quality Index ( $Q$ ) is defined by mathematic relation. By multiply the normalized stresses and shear stress in uniaxial compressive strength of intact rock masses, strength of rock mass is obtained in appropriate unit. [35] The state of stability of the wedge is then assessed through the factor of safety against roof failure, defined by:

$$FS = \frac{\tau_{HB}}{\tau} \quad (4)$$

In which  $\tau_{HB}$  is shear stress obtained from Hook and Brown approximate equations,  $\tau$  is shear stress applied on wedge surface, and FS is the factor of safety against roof failure. It is clear that when the factor of safety is below the defined level, wedge is unstable and requires support otherwise it is stable.

In previous section it was assumed that weight force was neutralized with two F reaction forces which are applied in vertical direction on lateral surfaces. But here it is assumed that applied force on shear surface make  $\beta$  angle with vertical direction. It is clear that when obtained FS is less than the previous state, the less one should be applied. In addition, the above conditions are investigated for two cases of asymmetric and symmetric falling wedges.

### 1-2. Symmetric falling roof wedge with non-vertical reaction force

In this case it is assumed that direction of weight force make  $\beta$  angle with directions of F forces applied on sliding surfaces. According to figure 4 it is clear that the maximum deviation of F-forces from vertical state is equal to  $\theta$ . Considering static equilibrium in vertical direction it can be written that:

$$W=2F\cos\beta \quad (5)$$

Then N-tensile normal force which is the vertical component of F reaction force is obtained from equation below:

$$N=-F\sin(\theta-\beta) \quad (6)$$

Also S-shear force which is the tangential component of F-force is based on Equation (7).

$$S=F\cos(\theta-\beta) \quad (7)$$

The other stages for obtaining factor of safety are the same as the previous section.

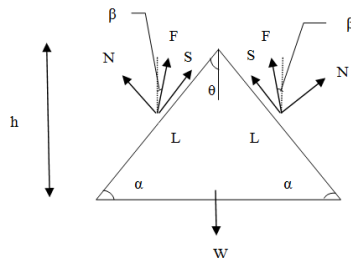


**Figure 4. Symmetric falling roof wedge with assumption of non-vertical direction of reaction forces applied on sliding surface**

## 2. Asymmetric falling roof wedge

### 2.1. Asymmetric falling roof wedge with vertical reaction force

The cross section of asymmetric falling wedge in the crown of an excavation which is formed by inclined asymmetric joint is shown in figure 5.

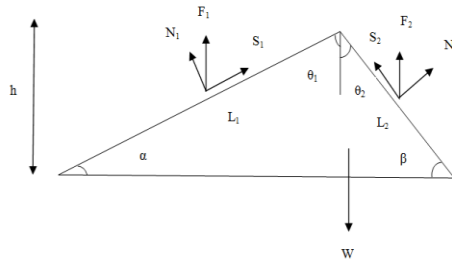


**Figure 5. Asymmetric falling roof wedge**

In this case two forces  $F_1$  and  $F_2$  exist on lateral sides:

$$F_1 + F_2 = W \quad (8)$$

Taking moment around the point of application of  $F_1$  force, the  $F_2$  force can be calculated and using Equation (8)  $F_1$  force is also obtained. In this case  $N_1$  and  $N_2$  tensile normal forces which are the vertical components of  $F_1$  and  $F_2$  forces are obtained as follows:

$$N_1 = -F_1 \sin \theta_1, \quad N_2 = -F_2 \sin \theta_2 \quad (9)$$

Moreover  $S_1$  and  $S_2$  shear forces which are the shear components of  $F_1$  and  $F_2$  forces are calculated based on Equation (10):

$$S_1 = F_1 \cos \theta_1, \quad S_2 = F_2 \cos \theta_2 \quad (10)$$

$\sigma_1$  and  $\sigma_2$  tensile normal stresses on lateral surfaces with the lengths of  $L_1$  and  $L_2$  are obtained as follow:

$$\sigma_1 = \frac{N_1}{L_1}, \quad \sigma_2 = \frac{N_2}{L_2} \quad (11)$$

$\tau_1$  and  $\tau_2$  shear stresses on lateral surfaces with the lengths of  $L_1$  and  $L_2$  are as follow:

$$\tau_1 = \frac{S_1}{L_1}, \quad \tau_2 = \frac{S_2}{L_2} \quad (12)$$

Also two factors of safety are obtained on two lateral sliding surfaces which for greater stability the minimum one should be considered:

$$FS_1 = \frac{\tau_{HB1}}{\tau_1}, \quad FS_2 = \frac{\tau_{HB2}}{\tau_2} \quad (13)$$

$$FS = \min (FS_1, FS_2) \quad (14)$$

In which  $\tau_{HB1}$  and  $\tau_{HB2}$  are shear stresses obtained from Hoek and Brown failure equations on lateral surfaces.



### 2.2. Asymmetric falling roof wedge with non-vertical reaction force

In this case  $F_1$  force makes  $\varphi$  angle with vertical direction. Equilibrium equations in horizontal and vertical directions are as follow:

$$\sum F_x = 0 \rightarrow F_1 \sin \varphi + N_2 \cos(90 - \beta) - S_2 \cos \beta = 0 \tag{15}$$

$$\sum F_y = 0 \rightarrow F_1 \cos \varphi + N_2 \sin(90 - \beta) + S_2 \sin \beta = W \tag{16}$$

Taking moment around each optional point, another equation is obtained based on  $F_1, S_2$  and  $N_2$  unknowns. After solution of the 3 equations 3 unknown  $F_1, S_2$  and  $N_2$  forces are calculated. It should be noted that  $N_2$  tensile normal force is the vertical component of  $F_2$  force and  $S_2$  shear force is the tangential component of  $F_2$  force.

Moreover  $N_1$  tensile normal force which is the vertical component of  $F_1$  reaction force and  $S_1$  shear force which is the tangential component of  $F_1$  force are obtained by Equations (17).

$$N_1 = -F_1 \cos(\theta_1 - \varphi) \quad , \quad S_1 = F_1 \sin(\theta_1 - \varphi) \tag{17}$$

The other stages for obtaining factor of safety are the same as the previous section.

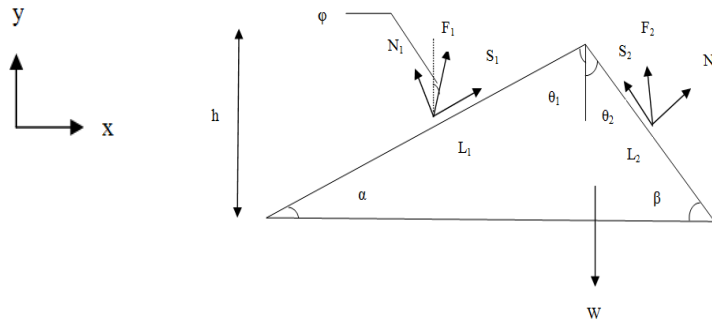


**Figure 6. Asymmetric falling roof wedge with assumption of non-vertical direction of reaction forces applied on sliding surface**

### 3. Vertical wedge

When at least one of the joint sets is vertical, vertical wedge form is made as figure 7. In this case there are two  $F_1$  and  $F_2$  force on lateral surface which is:

$$F_1 + F_2 = W \tag{18}$$

Taking moment around the point of application of  $F_2$  force, point  $o$  on the middle of the vertical side of wedge, the  $F_1$  force can be calculated and with regard to Equation (18)  $F_2$  force is also obtained.

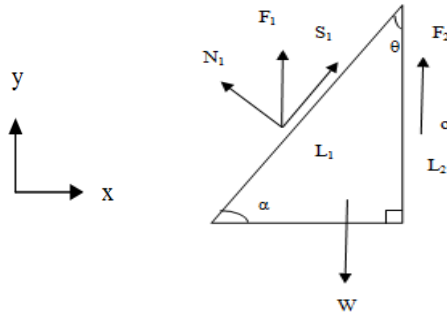


**Figure 7. Vertical wedge.**

$$\sum M_O = 0 \rightarrow F_1 = \frac{2}{3}w \quad , \quad F_2 = \frac{1}{3}w \quad (19)$$

It is clear that in this case  $N_1$  and  $N_2$  tensile normal forces which are the vertical components of  $F_1$  and  $F_2$  forces are obtained as the following equation:

$$N_1 = -F_1 \sin \theta \quad , \quad N_2 = 0 \quad (20)$$

Furthermore  $S_1$  and  $S_2$  shear forces which are the horizontal component of  $F_1$  and  $F_2$  forces are obtained as the following equation:

$$S_1 = F_1 \cos \theta \quad , \quad S_2 = F_2 \quad (21)$$

$\sigma_1$  and  $\sigma_2$  tensile normal stresses on lateral surface with the lengths of  $L_1$  and  $L_2$  will be as follow:

$$\sigma_1 = \frac{N_1}{L_1} \quad , \quad \sigma_2 = 0 \quad (22)$$

$\tau_1$  and  $\tau_2$  shear stresses on lateral surface with the lengths of  $L_1$  and  $L_2$  are also obtained.

$$\tau_1 = \frac{S_1}{L_1} \quad , \quad \tau_2 = \frac{S_2}{L_2} \quad (23)$$

Factors of safety obtained on two sliding surfaces are not necessarily equal that for the greater stability the minimum one is taken into account.

$$FS_1 = \frac{\tau_{HB1}}{\tau_1} \quad , \quad FS_2 = \frac{\tau_{HB2}}{\tau_2} \quad (24)$$

$$FS = \min (FS_1, FS_2) \quad (25)$$

In Equation (24)  $\tau_{HB1}$  and  $\tau_{HB2}$  are the shear stresses which are obtained from Hoek and Brown failure criterion on sliding surfaces.

#### 4. Inclined sliding wedge

The cross section of inclined sliding wedge in the crown of an excavation is shown in figure 8 in a way that the base of the wedge is its free surface.

Equilibrium equations in vertical and horizontal direction are as the following equations:

$$\sum F_x = 0 \rightarrow F_1 \sin \varphi + S_2 \sin \psi - N_2 \cos \psi = 0 \tag{26}$$

$$\sum F_y = 0 \rightarrow F_1 \cos \varphi + S_2 \cos \psi + N_2 \sin \psi = W \tag{27}$$

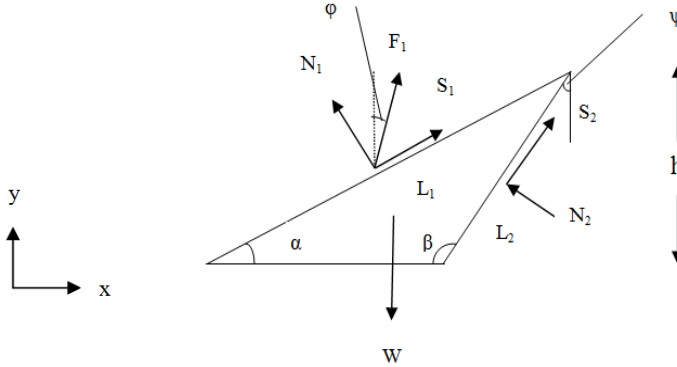


**Figure 8. Inclined sliding wedge**

Taking moment around each optional point, third equation is obtained based on  $F_1, S_2$  and  $N_2$  unknowns. After solution of the 3 equations 3 unknown  $F_1, S_2$  and  $N_2$  forces are calculated. It should be noted that  $N_2$  compressive normal force is the vertical component of  $F_2$  force and  $S_2$  shear force is the tangential component of  $F_2$  force.

Moreover  $N_1$  tensile normal force which is the vertical component of  $F_1$  force and  $S_1$  shear force which is the tangential component of  $F_1$  force are obtained as the following equations:

$$N_1 = -F_1 \sin(90 - (\alpha + \varphi)) \quad , \quad S_1 = F_1 \cos(90 - (\alpha + \varphi)) \tag{28}$$

$\sigma_1$  and  $\sigma_2$  tensile normal and compressive stresses on lateral surface with the lengths of  $L_1$  and  $L_2$  will be as follow:

$$\sigma_1 = \frac{N_1}{L_1} \quad , \quad \sigma_2 = \frac{N_2}{L_2} \tag{29}$$

$\tau_1$  and  $\tau_2$  shear stresses on sliding surface with the lengths of  $L_1$  and  $L_2$  are also as the following equation:

$$\tau_1 = \frac{S_1}{L_1} \quad , \quad \tau_2 = \frac{S_2}{L_2} \tag{30}$$

Factors of safety on two shear surfaces are obtained by Equations (31) which the minimum safety and stability should be taken into account:

$$FS_1 = \frac{\tau_{HB1}}{\tau_1} \quad , \quad FS_2 = \frac{\tau_{HB2}}{\tau_2} \quad , \quad FS = \min (FS_1, FS_2) \tag{31}$$

In which  $\tau_{HB1}$  and  $\tau_{HB2}$  are the shear stresses which are obtained from Hoek and Brown failure criterion on shear surfaces.

## Field observations

To clarify stability analysis of wedge in the tunnel roof by limiting equilibrium analytical method some examples are given. Condition for wedge formation in tunnel crown based on observations in New York City and Washington D.C are provided in Table 1 [36].

**Table 1. Condition for wedge formation in tunnel crown based on observations in New York City and Washington D.C**

Group	Dip angle $\alpha$ , degree	Half angle $\theta$ , degree
1	0-30	90-60
2	30-45	60-45
3	45-60	45-30
4	60-75	30-15
5	75-90	15-0

In addition to the rock wedges that tend to slide out of the sidewalls, there is a tendency for large wedges to slide and separate along continuous, planar surfaces in the crown of the tunnels. In rock in which the discontinuities are irregular, large deep wedges can only fail by shearing through irregularities, thus only small wedges require support (Group 1), whereas in rock containing steeply dipping sheared surfaces, much larger wedges must be supported (Group 4).

Here, observed wedges with the width of  $B=3\text{m}$ ,  $6\text{m}$  are considered. The rock is the Gneiss with uniaxial compressive strength of 100 MPa. Rock mass based on Q-Barton classification has the NGI rating = 0.156 so rock mass with fair quality (NGI rating: 1) and poor quality (NGI rating: 0.1) which are the upper and lower limit are investigated.

For the Gneiss rock normalized approximate equations of Hoek and Brown failure criterion for intact rock and jointed rock masses are as follow:

$$\tau_n = 0.346 (\sigma_n + 0.0002)^{0.7} \quad \text{for NGI rating: 1} \quad (32)$$

$$\tau_n = 0.203 (\sigma_n + 0.0001)^{0.686} \quad \text{for NGI rating: 0.1} \quad (33)$$

In which  $\tau_n$  and  $\sigma_n$  are normalized shear and normal stresses, respectively. Rock mass strength is obtained by multiplying the stresses and shear strength in uniaxial compressive strength of 100 MPa. Shear stress chart against normal stress for NGI rating=1, 0.1 is given in figures 9 and 10. Calculations for symmetric and asymmetric falling wedges, vertical and sliding wedges are performed and the rest of the obtained results are summarized in related figures. It is clear that by considering  $FS=1.5$  for stability of wedges, wedges having factor of safety below the defined limit, mentioned above, are unstable and required support. It should be noted that

the used support can be shotcrete, rock bolt or combination of them. All of the applied angles are based on degree.

The range of specified  $\alpha$  angles for the case of symmetric falling wedge is shown in figure (11).

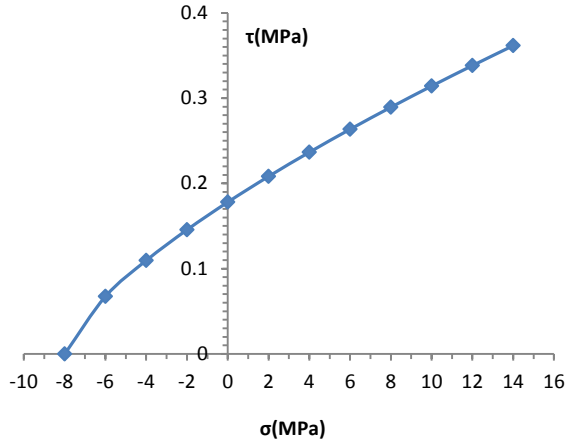


Figure 9. Shear stress chart against normal stress for NGI rating=1

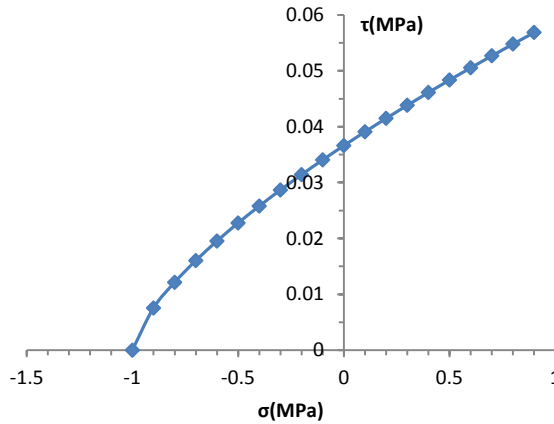
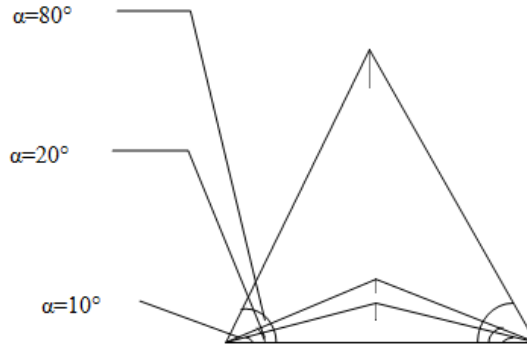


Figure 10. Shear stress chart against normal stress for NGI rating=0.1  
 a) Calculations and results for symmetric falling wedge:



**Figure 11. The range of specified  $\alpha$  angle for the case of symmetric falling roof wedge**

For example for half angle of  $\theta=40^\circ$ , width of  $B=3\text{m}$ , uniaxial compressive strength of  $\sigma_c=100\text{Mpa}$  and specific weight of  $2.38 \frac{T}{m^3}$  calculations are carried out as follow. Factors of safety in various  $\theta$  angles for wedges with the width of 3m and 6m are presented in figures 12 to 15.

$$h = 1.5 \times \tan 50 = 1.79 \text{ m} \quad , \quad w = \frac{\gamma \times B \times h}{2} = \frac{2.38 \times 3 \times 1.79}{2} = 6.38 \text{ T} \quad (34)$$

$$F = \frac{W}{2} = 3.19 \text{ T}, \quad L = \sqrt{1.5^2 + 1.79^2} = 2.33 \text{ m} \quad (35)$$

$$N = -F \sin 40 = -3.19 \sin 40 = -2.05 \text{ T} \quad (36)$$

$$S = F \cos 40 = 3.19 \cos 40 = 2.44 \text{ T}$$

$$\sigma = \frac{N}{L \times 1} = \frac{-2.05}{2.33 \times 1} = -0.88 \frac{T}{m^2} \quad (37)$$

$$\tau = \frac{S}{L \times 1} = \frac{2.44}{2.33 \times 1} = 1.049 \frac{T}{m^2}$$

$$\tau_n = 0.346 (\sigma_n + 0.0002)^{0.7} \text{ for NGI rating : 1} \quad ,$$

$$\sigma_c = 10000 \frac{T}{m^2} \quad (100 \text{ Mpa}) \quad (38)$$

$$\begin{aligned} \frac{\tau_{HB}}{10000} &= 0.346 \times \left( \frac{-0.88}{10000} + 0.0002 \right)^{0.7} \rightarrow \tau_{HB} = 5.94 \frac{T}{m^2} \quad , \quad FS = \frac{\tau_{HB}}{\tau} \\ &= \frac{5.94}{1.049} = 5.67 \end{aligned} \quad (39)$$

In which for  $\text{NGI}=0.1$  and  $\sigma_c=100\text{Mpa}$  the values of  $\tau_{HB} = 0.86 \frac{T}{m^2}$  and  $FS = 0.82$  are obtained. In the above calculations  $h$  is the height of wedge,  $w$  is the weight of wedge,  $\gamma$  is the specific weight of rock mass and  $B$  is the width of wedge.

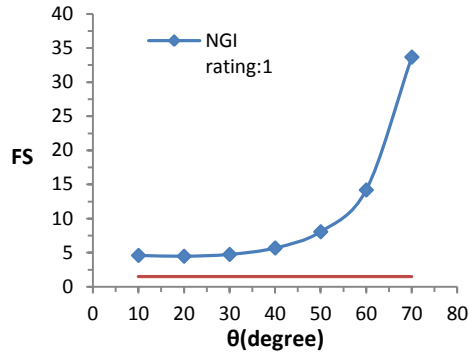


Figure 12. Factors of safety in various  $\theta$  angles for the width of 3m in the case of symmetric wedge

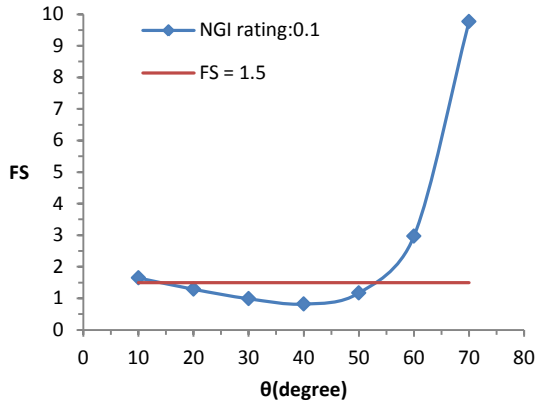
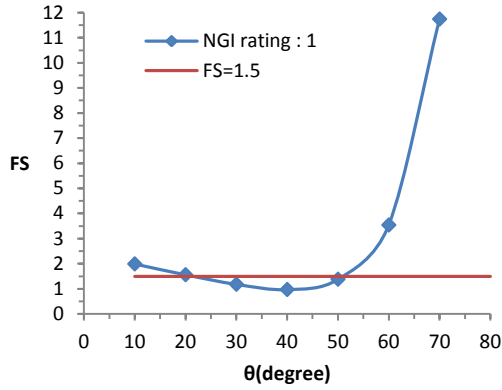
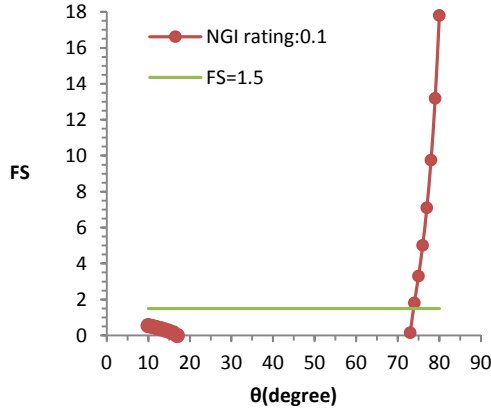


Figure 13. Factors of safety in various  $\theta$  angles for the width of 3m in the case of symmetric wedge



**Figure 14. Factors of safety in various  $\theta$  angles for the width of 6m in the case of symmetric wedge**



**Figure 15. Factors of safety in various  $\theta$  angles for the width of 6m in the case of symmetric wedge**

If it is assumed that weight force only causes the shear force on lateral surface of wedge,  $\frac{w}{2l}$  chart against half angle for the width of 3m will be as figure 16. As seen in figure 16 the shear stress due to weight on lateral surfaces decrease with the increase of the half angle of wedge.



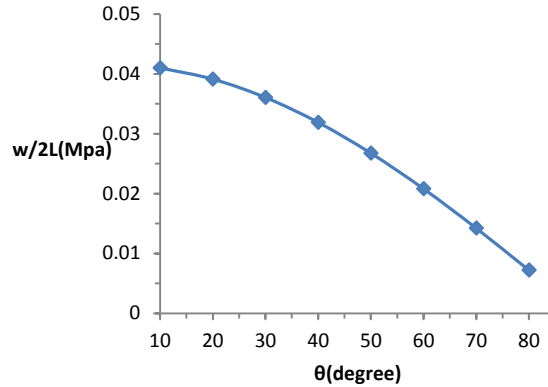


Figure 16.  $\frac{w}{2L}$  chart against half angle for the width of 3m

### b) Calculations and results for symmetric falling wedge with assuming the non-vertical direction of reaction forces on shear surfaces

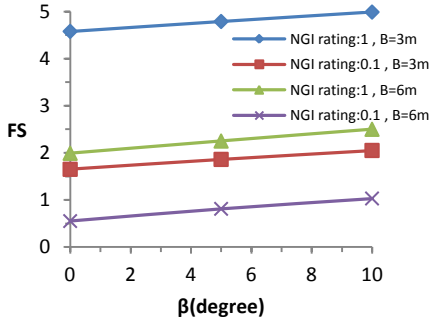
Up to now the obtained results for factor of safety was based on the assumption that applied F-forces is vertical on shear surface of symmetric falling wedge. Following that the obtained results of applied F-force deviation on shear surface are presented.

It is clear that the minimum factor of safety of the mentioned states, are taken into account. For symmetric wedge all cases are considered. It should be noted that the  $\beta=0$  for the case of symmetric wedge indicates the no deviation of applied F-force on the shear surface (vertical apply of force). All of angles are based on degree as previously mentioned.

For example for half angle  $\theta=60^\circ$ ,  $\beta=10^\circ$ , the width of 3m, the uniaxial compressive strength of 100 Mpa and specific weight of  $2.38 \frac{T}{m^3}$  calculations is performed. Variation of the factor of safety against  $\beta$  angle for  $\theta=10^\circ$  to  $\theta=80^\circ$  is given in figures 17 to 25 and finally factors of safety in various  $\theta$  angles is presented in figure 25 for the width of 3m and 6m in the case of symmetric falling wedge. Presented factors of safety are the minimum ones.

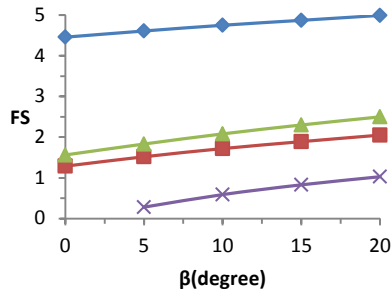
For this case the values of  $h = 0.866$  ,  $w = 3.09 T$  ,  $F = 1.57 T$  ,  $L = 1.73m$  was obtained based on Equations (34) and (35). Moreover normal and shear component of  $N = -1.20 T$  and  $S = 1.01 T$  also  $\sigma = -0.69 \frac{T}{m^2}$  and  $\tau = 0.58 \frac{T}{m^2}$  are obtained using Equations (36) and (37) in which finally

factors of safety  $FS = 11.35$  و  $2.79$  for  $NGI=1$  and  $0.1$  are obtained by Equations (39).



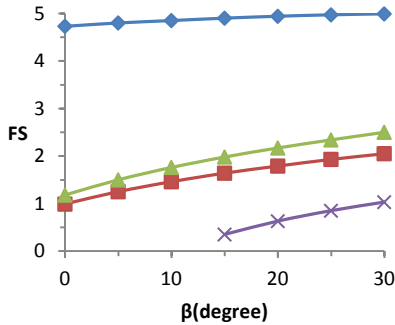
(Figure 17.)

**Figure 17. Variation of the factors of safety against  $\beta$  angle for  $\theta=10^\circ$  in the case of symmetric falling wedge**



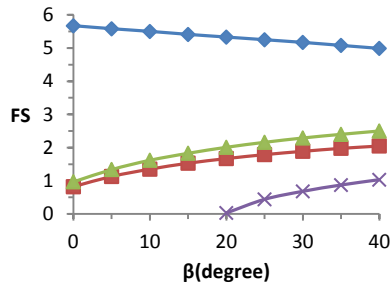
(Figure 18)

**Figure 18. Variation of the factors of safety against  $\beta$  angle for  $\theta=20^\circ$  in the case of symmetric falling wedge**



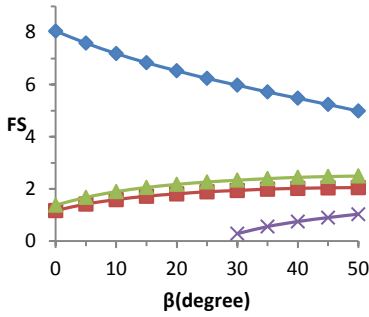
(Figure 19.)

**Figure 19. Variation of the factors of safety against  $\beta$  angle for  $\theta=30^\circ$  in the case of symmetric falling wedge**



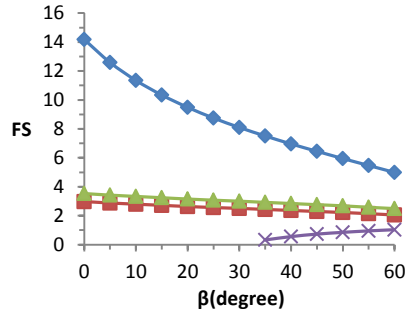
(Figure 20)

**Figure 20. Variation of the factors of safety against  $\beta$  angle for  $\theta=40^\circ$  in the case of symmetric falling wedge**



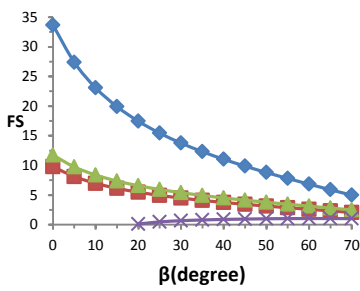
(Figure 21)

Figure 21. Variation of the factors of safety against  $\beta$  angle for  $\theta=50^\circ$  in the case of symmetric falling wedge



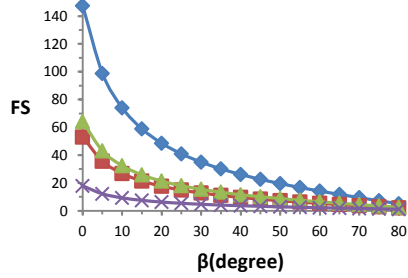
(Figure 22)

Figure 22. Variation of the factors of safety against  $\beta$  angle for  $\theta=60^\circ$  in the case of symmetric falling wedge



(Figure 23)

Figure 23. Variation of the factors of safety against  $\beta$  angle for  $\theta=70^\circ$  in the case of symmetric falling wedge



(Figure 24)

Figure 24. Variation of the factors of safety against  $\beta$  angle for  $\theta=80^\circ$  in the case of symmetric falling wedge

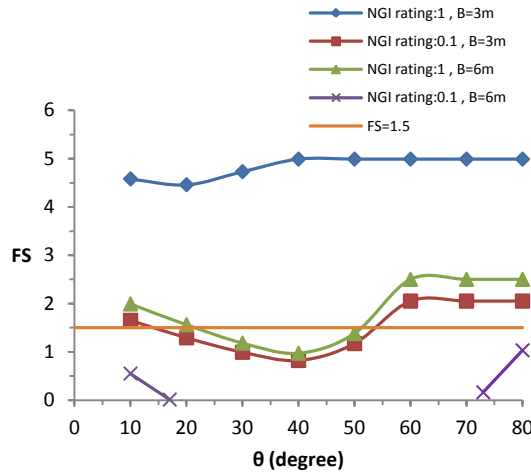


Figure 25. Factors of safety in various θ angles for the width of 3m and 6m in the case of symmetric falling wedge

c) Calculations and results for vertical wedge

The range of specified α angles for the case of vertical wedge is shown in Figure 26. For example for α=30°, width of B=3m, uniaxial compressive strength of σ<sub>c</sub>=100Mpa and specific unit weight of 2.38  $\frac{T}{m^3}$  calculations is performed. The factors of safety for various α angles for wedges with the widths of 3 and 6m are presented in figures 27 to 30.

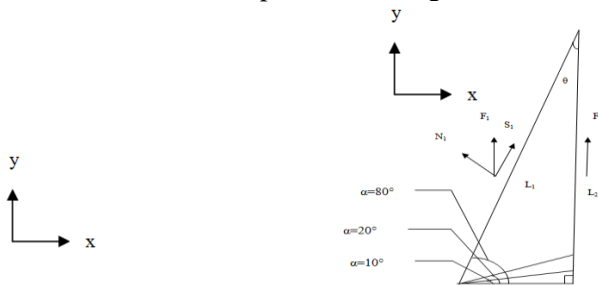
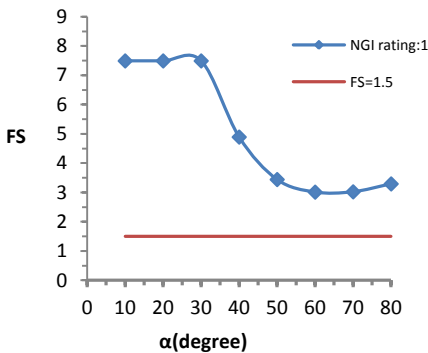


Figure 26. The range of specified α angle for the case of vertical wedge.

For this case this values  $h = 1.73m$ ,  $w = 6.18 T$ ,  $L_1 = 3.46 m$ ,  $L_2 = h = 1.73 m$ ,  $F_1 = 4.12 T$  and  $F_2 = 2.06 T$  are obtained based on Equations (19).  $N_1 = -3.57 T$  and  $N_2 = 0$  tensile normal forces and  $S_1 = 2.06 T$  and  $S_2 = F_2 = 2.06 T$  shear forces also  $\sigma_1 = -1.03 \frac{T}{m^2}$  and  $\sigma_2 = 0 \frac{T}{m^2}$  tensile normal stresses,  $\tau_1 = 0.59 \frac{T}{m^2}$  and  $\tau_2 = 1.19 \frac{T}{m^2}$  shear

stresses are obtained based on Equations (20) to (23). Finally by replacing in the relations (24) and (25) factor of safety for  $NGI=1$  is obtained which is equal to 7.49. Also for  $NGI=0.1$  the value for factor of safety is not obtained which indicates the failure. As shown in Figure 27 for  $\alpha$  angle to 30 degree factors of safety is independent from the  $\alpha$  angle. Then with the increase of  $\alpha$  angle the factor of safety decreases and again after the angle of 70 degree increases. In Figure 28 it is illustrated that for  $\alpha$  angles to 25 degree factors of safety is independent from  $\alpha$  angle. After that it will decrease with the increasing of  $\alpha$  angle. In  $\alpha$  angle from 30 to 60 degree failure occurred and after that it will increase with the increasing of  $\alpha$  angle. In Figure 30 shown that from  $\alpha$  angles to 10 degree factors of safety is independent from the  $\alpha$  angle. After that failure occurred. If  $\alpha$  angle greater than 75 degree the factor of safety increases with the increasing of  $\alpha$  angle.

By extrapolation of factor of safety charts against  $\alpha$  angle by the use of cubic functions with the width of 3m and  $NGI$  rating: 1 and the width of 6m and  $NGI$  rating: 1, 0.1 critical vertical wedges can be predicted. This is shown in Figure 31. The used cubic equations are as Equation (40) to (42). As shown in Figure 31 chart of factor of safety against  $\alpha$  angle for  $NGI:1$ ,  $B=3m$  and  $NGI:0.1$ ,  $B=6m$  are similar and the minimum factors of safety is in the range of  $\alpha$  angle equal 60 to 70 degree. Also chart of factor of safety against  $\alpha$  angle for  $NGI:0.1$ ,  $B=3m$  and  $NGI:1$ ,  $B=6m$  are the same and the minimum factors of safety is in the range of  $\alpha$  angle equal 40 to 50 degree.



(Figure 27)

**Figure 27. Factors of safety in various  $\alpha$  angles for the width of 3m in the case of vertical wedge  $NGI:1$**

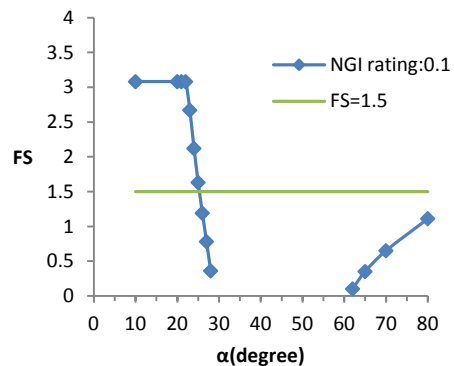


(Figure 28)

**Figure 28. Factors of safety in various  $\alpha$  angles for the width of 3m in the case of vertical wedge  $NGI:0.1$**

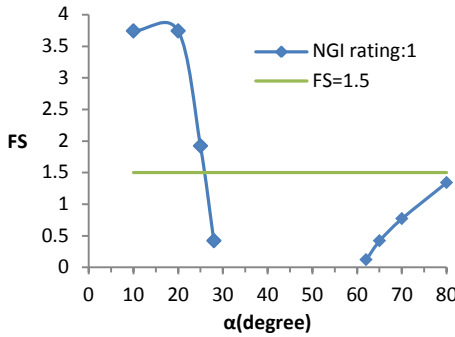


(Figure 29)

Figure 29. Factors of safety in various  $\alpha$  angles for the width of 6m in the case of vertical wedge NGI:1

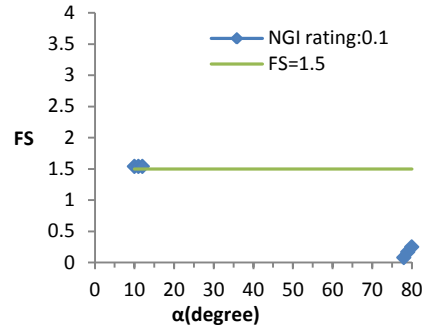


(Figure 30)

Figure 30. Factors of safety in various  $\alpha$  angles for the width of 6m in the case of vertical wedge NGI:0.1

$$y = -0.00021x^3 + 0.0355x^2 - 1.866x + 29.41 \text{ for NGI rating:0.1, } B=3\text{m} \quad (40)$$

$$y = -0.00016x^3 + 0.0276x^2 - 1.482x + 23.75 \text{ for NGI rating : 1, } B=6\text{m} \quad (41)$$

$$y = 0.000027x^3 - 0.003x^2 + 0.0568x + 1.2475 \text{ for NGI rating :0.1, } B=6\text{m} \quad (42)$$

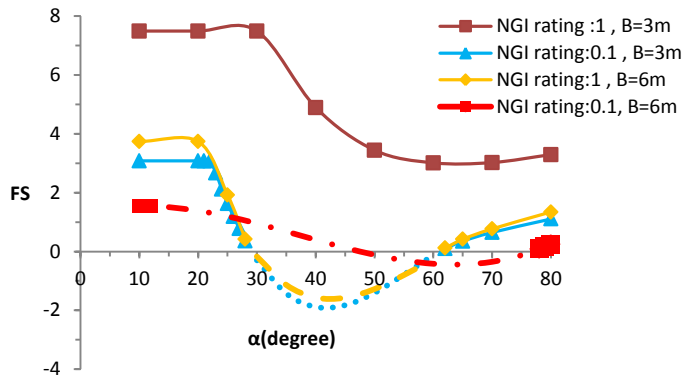


Figure 31. The prediction of critical state of the vertical wedge

## Conclusions

The stability of wedges formed around underground excavations in blocky and jointed rock masses is a common problem in rock engineering. The wedges are formed by intersecting discontinuities and the free face created through excavation of an underground opening. Under the influence of gravity and other forces, roof and wall wedges may fail either by falling, sliding or rotating out of their sockets. The factors that control wedge stability include geometry (the size, shape and spatial location of a wedge), the strength characteristics of the discontinuity planes that create the wedge, and stresses within the rock mass. Most existing algorithms for underground wedge stability analysis assume that stresses are sufficiently low and can therefore be ignored. This is fine for wedges in low in situ stress environments, such as those encountered in shallow excavations. The stability of a wedge in the roof of an excavation is an example. Such a wedge fails by falling under the influence of self-weight. Compared with other methods of stability analysis presented in the introduction, Using the Hoek and Brown failure criterion, which encompasses a wide range of different rocks and have a good agreement with field observations, and the simplicity of this method is its advantages. The Hoek-Brown failure criterion for rock masses is widely accepted and has been applied in a large number of projects around the world. In general, it has been found to be satisfactory. These relationships have been found useful in preliminary design calculations for slopes and underground excavations in jointed rock. This approach permits rapid assessments of rock mass strength and stability of structures such as tunnel to be made in the early stages of project development before extensive field test programs or trial excavation studies have been undertaken. Based on the field investigations, the wedges stability of a large underground excavation is studied in this paper with limiting equilibrium analytical method and by use of Hoek and Brown failure criterion in four states (symmetric and asymmetric falling, vertical and sliding wedges). Since the estimation of support requirements to stabilize potentially removable blocks surrounding underground openings is of prime importance, appropriate corresponding of field observations with analytical method show that this method can be used for rational design of such structures. It is natural that, since the NGI rating of rock mass equal to 0.156, results for NGI rating: 0.1 are of better correspondence and agreement with the field observations.

## References

1. Bray J. W., "Unpublished note", Imperial College, London (1979).
2. John K. W., "Graphical stability analysis of slopes in jointed rock", *J. Soil Mech. Found Div (ASCE)*. 94(2) (1968) 497-526.
3. Londe P., Vigier G., Vormeringer R., "Stability of rock slopes, a three-dimensional study", *J. Soil Mech. Found. Div. (ASCE)* 95 (1) (1969) 235-62.
4. Hendron A. J., Cording E. J., Aiyer A. K., "Analytical and graphical methods for the analysis of slopes in rock masses", Technical Report GL-80-2, US Army Engineers Nuclear Cratering Group, Livermore, CA, (1980) 1-55.
5. Hoek, E. T., Bray J. W., "Rock slope engineering", 3rd ed. London, England: Institute of Min and Metallurgy (1981) 275-342.
6. Warburton P. M., "Vector stability analysis of an arbitrary polyhedral rock block with any number of free faces", *Int. J. Rock Mech. Min. Sci. Geomech. Abstr*;18(5) (1981) 415-27.
7. Priest S. D., "Hemispherical projection methods in rock mechanics ", London: George Allan & Unwin (1985) 75-84.
8. Goodman R. E, Shi GH., "Block theory and its application to rock engineering, London: Prentice-Hall (1985) 147-162.
9. Chan H. C., Einstein H. H., "Approach to complete limit equilibrium analysis for rock wedges-the method of artificial supports", *Rock Mech*;14(2) (1981) 59-86.
10. Mauldon M., Goodman R. E., "Vector analysis of keyblock rotation", *J. Geotech Geoenviron Eng (ASCE)*;122(12) (1996) 976-87.
11. Tonon F., "Generalization of Mauldon's and Goodman's analysis of keyblock rotations", *J Geotech Geoenviron Eng (ASCE)* 124 (10) (1998) 913-22.
12. Sofianos A. I., "Stability of wedges in tunnel roofs", *Int J Rock Mech Min Sci Geomech Abstr*, 23 (2) (1986) 119-30.
13. Sofianos A. I., Nomikos P, Tsoutrelis C. E., "Stability of symmetric wedge formed in the roof of a circular tunnel: nonhydrostatic natural stress field. *Int J Rock Mech Min Sci.*, 36 (1999) 687-91.
14. Nomikos P., Sofianos A. I., Tsoutrelis C. E., "Symmetric wedge in the roof of a tunnel excavated in an inclined stress field", *Int J Rock Mech Min Sci.*, 39 (2002) 59-67.
15. Hudson J. A., Harrison J. P., "Engineering rock mechanics: an introduction to the principles", 4th ed.. Amsterdam: Elsevier (2005).
16. Rocscience, *Unwedge Theory Manual-Factor of Safety Calculations* /[http://www.rocscience.com/downloads/unwedge/unwedge\\_theory.pdf](http://www.rocscience.com/downloads/unwedge/unwedge_theory.pdf). (2009).
17. Asadollahi P., "Stability analysis of a single three dimensional rock block: effect of dilatancy and high-velocity water jet impact", PhD dissertation, University of Texas: Austin (2009).



18. Tonon F., "Analysis of single rock blocks for general failure mode under conservative and non-conservative forces", *IntJ Numer Anal Methods Geomech*;31(14) (2007) 1567-608.
19. Tonon F., Asadollahi P., "Validation of single rock block stability analysis (BS3D) for wedge failure", *IntJ Rock MechMin. Sci.*, 45, (2008) 627-37.
20. Asadollahi P., Tonon F., "Definition of factor of safety for rock blocks", *International Journal of Rock Mechanics & Mining Sciences* 47 (2010) 1384-1390.
21. Wang Y. J., Yin J. H., "Wedge stability analysis considering dilatancy of discontinuities", *Rock Mech., Rock Eng.*, 35 (2) (2002) 127-37.
22. Chen Z. Y., "A generalized solution for tetrahedral rock wedge stability analysis", *Int J Rock Mech., Min Sci.*, 41, (2004) 613-28.
23. Yeung M. R., Jiang Q. H., Sun N., "Validation of block theory and three-dimensional discontinuous deformation analysis as wedge stability analysis methods", *Int J Rock Mech., Min Sci.*, 40, (2003) 265-75.
24. Low B. K., "Reliability analysis of rock wedges", *J Geotech Geoenviron Eng.*, 123 (6) (1997) 498-505.
25. Park H., West T. R., "Development of a probabilistic approach for rock wedge failure", *Eng Geol.*, 59 (2001) 233-51.
25. Park H. J., West T. R., Woo I., "Probabilistic analysis of rock slope stability and random properties of discontinuity parameters", *parameters, Interstate High-way 40, Western North Carolina, USA. Eng., Geol.*, 79 (2005) 230-50.
26. Jimenez-Rodriguez R., Sitar N., "Rock wedge stability analysis using system reliability methods", *Rock Mech., Rock Eng.*, 40 (4) (2007)419-27.
27. Low B. K., "Reliability analysis of rock slopes involving correlated non-normals. *Int J Rock Mech Min Sci*;44(6):922-35(2007).
28. Li DQ, Zhou CB, Lu WB, Jiang QH. A system reliability approach for evaluating stability of rock wedges with correlated failure modes. *Comp Geotech*;36(8):1298-307(2009).
29. Duncan CW, Christophere WM. *Rock slope engineering: civil and mining*. 4rd ed. New York: Spon Press; (2004).
30. Jiang Q, Liu X, Wei W, Zhou Ch . A new method for analyzing the stability of rock wedges. *International Journal of Rock Mechanics & Mining Sciences* 60 , 413-422(2013).
31. Mirzaeian, F., K.Shahriar .,M.Sharifzadeh,"Tunnel Probabilistic Structure Analysis Using the FORM",*Journal of Geological Research,Hindawi Publishing Corporation, Article ID 3947,PP. 1-10(2015).*
32. Curran, J.H., B.Corkum ., R.E.Hammah,"Three-dimensional Analysis of Underground Wedges under the Influence of Stresses",<http://www.rocscience.com/documents/pdfs/uploads/7776.pdf>,PP.1-7(2015).
33. Budiman, R.C., R.Pratama ., D.Muslim and I.Sophian,"Design Analysis of Tunnel Portal in Pasi Jawa L250 Pongkor's GMBU Underground Mine PT. Aneka Tabbang Tbk.,10<sup>th</sup> Asian Regional Conference of IAEG,PP.1-6(2015)

34. Brady, B.H.G, Brown, E.T., " Rock Mechanics for Underground mining", George Allen &Unwin (publishers) Ltd,PP. 352-364(1992).
35. Hoek, E., Brown, E.T, "Underground excavations in rock", The Institution of Mining and Metallurgy,PP. 115-127(1980).
36. Cording, Edward.J., Mahar, James W., Brierley, G. S., "Observation for shallow chambers in rock",Proceedings of the International Symposium,Zurich, April 4-6,PP. 485-508 (1977).